Time-resolved small angle neutron scattering measurements of asphaltene nanoparticle aggregation kinetics in incompatible crude oil mixtures

Thomas G. Mason[a]
Corporate Strategic Research, ExxonMobil Research and Engineering Company, Annandale, New Jersey 08801

Min Y. Lin
Center for Neutron Research, National Institute of Standards and Technology, Gaithersburg, Maryland 20899

We use time-resolved-small angle neutron scattering to study the kinetics of asphaltene nanoparticle aggregation in incompatible crude oil mixtures. We induce asphaltene aggregation by mixing asphaltene-rich Syrian crude oil (SACO) with a paraffinic British crude oil and observe the scattered neutron intensity, I, as a function of wave number, q, over times, t, ranging from twenty minutes to about a week. We observe a growth in I at low q as the nanoscale asphaltenes agglomerate into microscale aggregates and interpret this growth as an increase in surface scattering from the aggregates. We fit $I(q,t)$ to an empirical model and measure the growth in the power-law exponent, α, associated with the low-q logarithmic slope of $I(q)$. We define a time, τ_α, associated with the first appearance of the aggregates when $\alpha > 3$; τ_α increases as a function of the volume fraction, ϕ_m, of SACO in the mixture. The surface scattering intensity initially increases and then saturates at long times when the aggregate structures no longer evolve at the length scales we probe. Based on this saturation, we define a time scale, τ_I, which is larger than τ_α but has essentially the same dependence on ϕ_m. We interpret $\tau_\alpha(\phi_m)$ and $\tau_I(\phi_m)$ in terms of a simple aggregation model based on diffusion-limited kinetics and a repulsive potential barrier that models the effective solvent quality. © *2003 American Institute of Physics.* [DOI: 10.1063/1.1572457]

I. INTRODUCTION

One of the least understood aspects of the incompatibility of crude oils is the dynamic process of asphaltene aggregation. When a heavy oil containing thermally dispersed aromatic asphaltenes is mixed with a lighter, nonpolar, paraffinic oil, the interactions between the asphaltenes can become strongly attractive, leading to asphaltene aggregation.[1–4] Typically, the initial convective shear mixing is completed rapidly compared to the time scales associated with the asphaltene aggregation. In this case, the asphaltene particles diffuse and stick together to form aggregates when the depth of the attractive well in their interaction potential significantly exceeds thermal energy. Based on our knowledge of the aggregation kinetics of model colloids, such as polystyrene spheres[5] and emulsion droplets,[6] we expect that the kinetics of the aggregation process may be dependent on the concentration of the asphaltenes present in the mixture and also on the stabilizing repulsive barrier and the shorter-range attractive well in a hypothetical average interaction potential. In fact, the very idea of using a single pair inter-action potential to describe the average interactions between a wide variety of differently shaped asphaltene particles in crude oil mixtures may be too simplistic since the interactions may arise from different sources and may be orientation dependent. However, the traditional approach to explaining aggregation from a single interaction potential makes simple quantitative analysis possible, and might work even for complex practical systems such as crude oil mixtures. In crude oil mixtures, both the concentration of asphaltenes and the strength of the average interparticle attraction may change as a function of the volume fraction of mixing of the asphaltene-containing oil, ϕ_m, there may be a wide range of time scales over which the aggregation can take place.

Recently, small angle neutron scattering (SANS) has been used to examine the static structure of asphaltenes in incompatible crude oil mixtures systematically long after the oils have been blended.[7] This work represents a direct approach for detecting and quantifying how much paraffinic oil can be added to an asphaltenic oil before asphaltene aggregation occurs for native (i.e., undeuterated) crude oils, despite significant incoherent scattering from the high density of hydrogen nuclei. In particular, the SANS intensity analysis method discussed in this work permits the quantification of the degree of asphaltene aggregation either from the presence of surface scattering from the aggregates or from a reduction in the scattering from the colloidal scattering signature of asphaltene nanoparticles. Applying SANS directly to crude oil mixtures and using the systematic analysis method represents a significant advance over other SANS studies of asphaltenes in deuterated solvents.[8–11]

In this article, we present neutron scattering measurements of the aggregation time scales for an incompatible mixture of asphaltene-rich Syrian crude oil (SACO) and paraffinic British crude oil (BPCO) crude oils as a function of the mixing volume fraction. Rather than studying the static

---
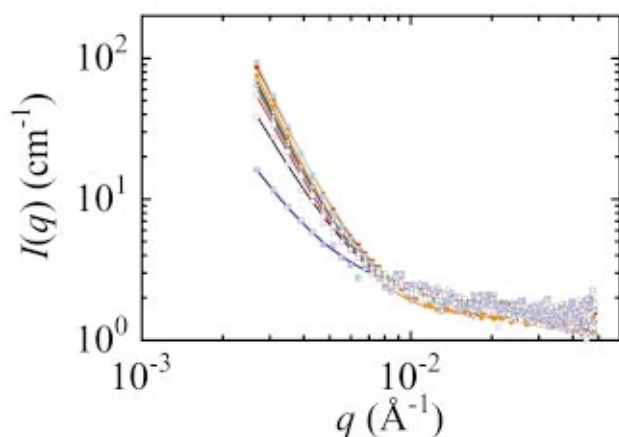
[a]Electronic mail: thomas.g.mason@exxonmobil.com

FIG. 1. (Color) Measured scattered neutron intensity, I, as a function of wave number, q, for a SACO/BPCO crude oil mixture at a SACO volume fraction of $\phi_m=0.1$ at times (in order from bottom to top) of $t=600$ s (blue crossed open squares), 3600 s (black open circles), 1.1×10^4 s (magenta open squares), 1.9×10^4 s (light green open triangles), 2.8×10^4 s (purple open diamonds), 3.7×10^4 s (dark green inverted triangles), 2.6×10^5 s (orange solid diamonds), 4.8×10^5 s (light blue solid squares), and 6.0×10^5 s (red solid circles) following mixing. The open symbols represent early time measurements on the same sample immediately after mixing, and the solid symbols represent different samples that were premixed days before the measurements. The solid lines are fits to the data using Eq. (1).

structure long after mixing, we use time-resolved-SANS (TR-SANS) to study the aggregation process by measuring the time evolution of the scattered neutron intensity, I, as a function of wave number, q, after mixing for several different ϕ_m. Using our previously developed analytical method[7] that separates out contributions to the scattering from unaggregated asphaltene particles and larger asphaltene aggregates, we are able to track the formation, growth, and saturation of the asphaltene aggregates following the mixing of the two crude oils. Using this method, we parameterize the strong increase in $I(q)$ at low q resulting from the surface scattering as the aggregates grow. This provides quantitative measures of the time scales associated with the first recognizable aggregates and also time scales associated with the cessation of evolution of the aggregate structures over the
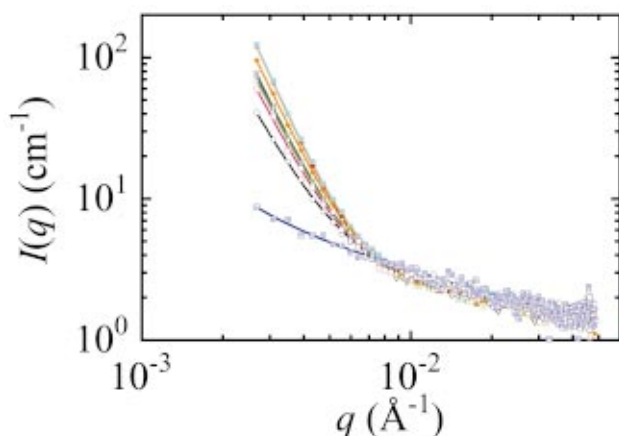
length scales we probe. In order to understand the measured time scales, we have developed a simple scaling model for the aggregation time based on diffusion-limited aggregation that broadly explains the measurements and may be used to estimate the aggregation time for other incompatible crude oil mixtures.

II. EXPERIMENT

To obtain TR-SANS measurements of the aggregation kinetics over a wide range of time scales, we have used essentially two different sets of samples. To determine the long-time behavior over many days while conserving neutron beam time, we have premixed several sets of crude oil mixtures of SACO and BPCO at identical $\phi_m=0.1$, 0.2, 0.3, and 0.4 on different days preceding the measurements. These samples have been loaded into individual 2 mm quartz cells after shaking to redisperse any asphaltene aggregates that may have settled. To determine the short-time behavior over time scales less than roughly one day, we made a single set of mixtures for the same set of ϕ_m, loaded them into 2 mm

FIG. 2. (Color) Scattered neutron intensity, I, as a function of wave number, q, for a SACO/BPCO crude oil mixture at $\phi_m=0.2$. The symbols and lines have the same meaning as in Fig. 1.
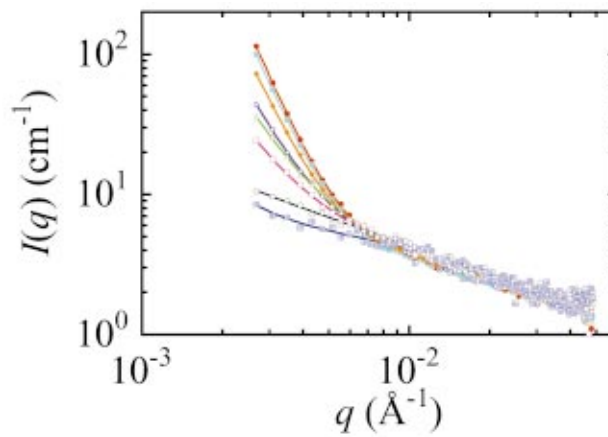

FIG. 3. (Color) Scattered neutron intensity, I, as a function of wave number, q, for a SACO/BPCO crude oil mixture at $\phi_m=0.3$. The symbols and lines have the same meaning as in Fig. 1.
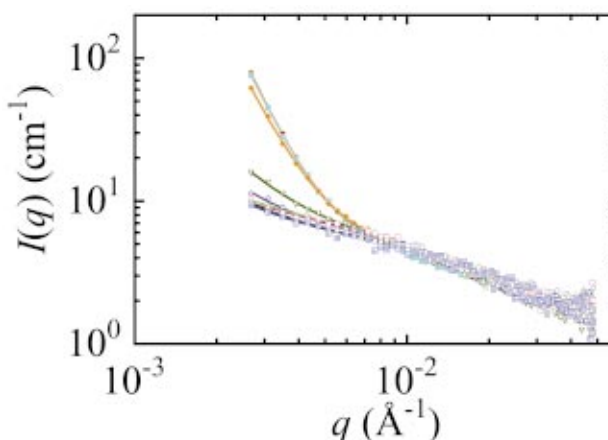

FIG. 4. (Color) Scattered neutron intensity, I, as a function of wave number, q, for a SACO/BPCO crude oil mixture at $\phi_m=0.4$. The symbols and lines have the same meaning as in Fig. 1, except the dark green inverted triangles refer to time $t=8.6\times10^4$ s.
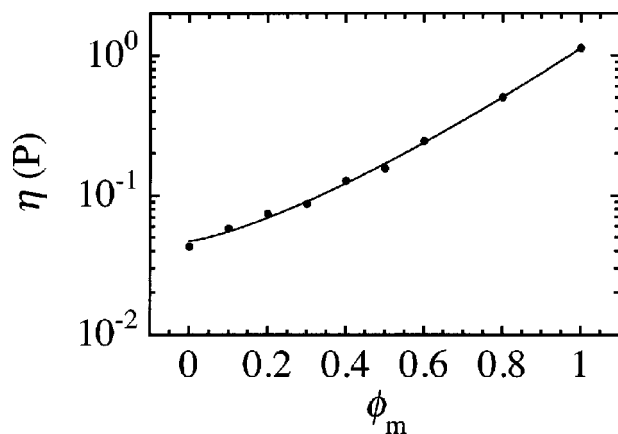
FIG. 5. Steady shear viscosity of SACO/BPCO crude oil mixtures measured at a shear rate of 200 s^{-1} as a function of the volume fraction of SACO oil, ϕ_m. The solid line represents a fit to the data using Eq. (12).
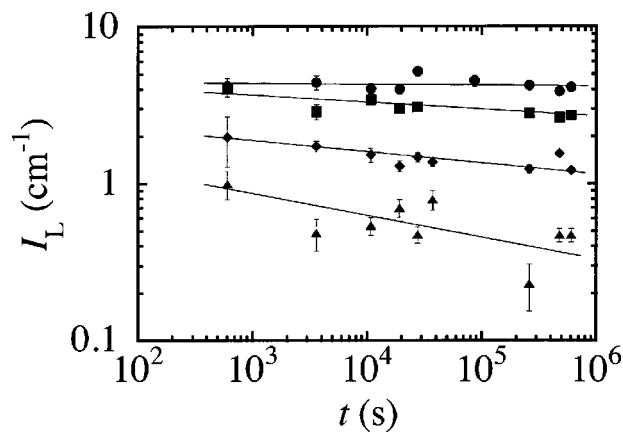

FIG. 6. The temporal dependence of the intensity of the Lorentzian fitting term, I_L, obtained from the fits of the data in Figs. 1–4. The mixing volume fractions are $\phi_m = 0.1$ (triangles), 0.2 (diamonds), 0.3 (squares), and 0.4 (circles). The solid lines guide the eye.

quartz cells, placed the cells in the SANS automated sample cell holder, and immediately commenced the scattering measurements. The SANS measurements were performed at the NIST Center for Neutron Research using the 30 m NG7 instrument.

Since we wish to detect the first appearances of surface scattering from aggregates, we set the array detector distance to correspond to the lowest possible q range, 0.0027 Å^{-1} $\leqslant q \leqslant 0.050$ Å^{-1} at the neutron wavelength is fixed at $\lambda = 5$ Å. The minimum data collection time to obtain reasonable statistics was about 20 min, essentially the smallest time at which we could observe $I(q)$. Similarly, each measured $I(q)$ represents a temporal average of scattering from the asphaltene structures over a 20 min period. The entire experiment has been carried out at room temperature, $T \approx 23$ °C.

Because we expect the time scales of aggregation to depend on the viscosity of the crude oil mixture, η, we have measured the steady shear viscosity of SACO/BPCO mixtures as a function of ϕ_m. The samples are mixed at room temperature and immediately loaded into a concentric cylinder couette geometry on a strain controlled rheometer. We find that a shear rate of 200 s^{-1} is sufficiently large for the torque on the fixed inner cylinder to be measured at all ϕ_m, including low ϕ_m where the viscosity and torque are small. For each sample, the measurement takes only several hundred seconds, so this viscosity represents the short-time limit of a homogeneous mixture before asphaltenes have aggregated. Subsequent measurements of the viscosity at longer times show that it does not change appreciably for this mixture even after the aggregation has occurred.

III. RESULTS

We show the temporal evolution of $I(q)$ for SACO/BPCO mixtures at $\phi_m = 0.1$, 0.2, 0.3, and 0.4 in Figs. 1–4, respectively. The sample with the lowest $\phi_m = 0.1$ exhibits a rapid initial increase in the low-q scattering intensity followed by a saturation of $I(q)$ toward a final terminal shape at long times. The sample with the highest $\phi_m = 0.4$ exhibits an $I(q)$ that changes little at the earliest times we measure, increases significantly over in $I(q)$ at low q over a time of

roughly one day, and approaches a final terminal shape at the longest times we measure. The measurements for the other two ϕ_m in Figs. 2 and 3 lie systematically between these two extremes.

The measured dependence of the viscosity of the crude oil mixtures on the mixing volume fraction is shown by the points in Fig. 5. The light BPCO crude oil at $\phi_m = 0$ has a viscosity of $\eta = 4.4$ cP, whereas the heavy SACO crude oil at $\phi_m = 1$ has a viscosity of $\eta = 100$ cP. Between these two limits, the viscosity rises monotonically and increases more rapidly as $\phi_m \to 1$.

IV. ANALYSIS

In order to parameterize the behavior of $I(q)$ as a function of ϕ_m and time, t, we fit $I(q)$ using a model that has been applied to SACO/BPCO mixtures long after aggregation has taken place. The model assumes that the scattering arises from three distinct sources: constant incoherent scattering intensity, I_{incoh}, from the hydrogen nuclei, Lorentzian scattering from nanometer-scale unaggregated asphaltene particles, and surface scattering from significantly larger asphaltene aggregates. The functional form is:[7]

$$I(q) = I_{incoh} + I_L / (1 + q^2 \xi^2) + I_{surf}(q/q_1)^{-\alpha}, \quad (1)$$

where I_L represents the Lorentzian scattering intensity of the unaggregated asphaltene particles; ξ represents a correlation length associated with the size of the particles; I_{surf} represents the magnitude of the surface scattering intensity at the lowest wave number, $q_1 = 0.0027$ Å^{-1}, we probe; and α is the exponent associated with the logarithmic slope of the surface scattering at low q. This functional form does not attempt to extract the likely continuum of sizes of asphaltene structures that may occur during aggregation, but instead, lumps all of the contributions from the these structures into the third power-law surface scattering term.

The solid lines in Figs. 1–4 represent the fits to the SANS data using Eq. (1) where the background incoherent scattering intensity has been fixed to be $I_{incoh} \approx 1.3$ cm^{-1} based on scattering measurements at higher q where it is more clearly defined. For all mixing volume fractions and
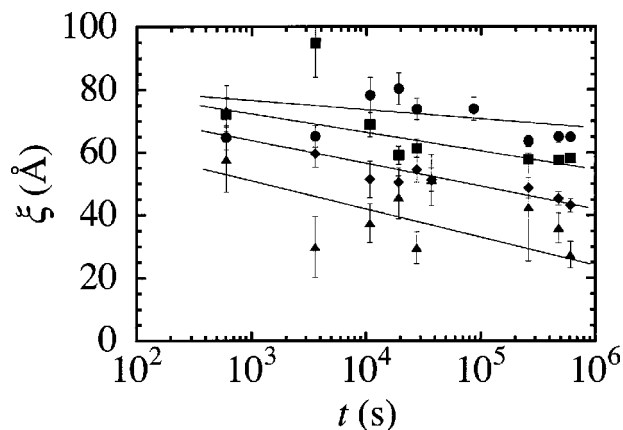
FIG. 7. The temporal dependence of the correlation length of the Lorentzian fitting term, ξ, obtained from the fits of the data in Figs. 1–4. The mixing volume fractions are $\phi_m = 0.1$ (triangles), 0.2 (diamonds), 0.3 (squares), and 0.4 (circles). The solid lines guide the eye.

FIG. 9. The temporal dependence of the intensity of the surface scattering, I_{surf}, obtained from the fits of the data in Figs. 1–4. The mixing volume fractions are $\phi_m = 0.1$ (triangles), 0.2 (diamonds), 0.3 (squares), and 0.4 (circles). The solid lines correspond to fits to the data using Eq. (2).

times, the fits in Figs. 1–4 agree very well with the data. We show the time dependence of the parameters associated with the Lorentzian term, I_L and ξ, in Figs. 6 and 7, respectively. The overall amplitude of the Lorentzian intensity in Fig. 6 increases with ϕ_m as more SACO asphaltenes are added to the mixture. Because the overall amplitude of I_L is low for $\phi_m = 0.1$, there is a significant scatter and it is difficult to precisely determine the evolution of I_L and ξ from the fits. Moreover, the limited q range increases the uncertainty in value of ξ. At $\phi_m = 0.2$ and 0.3, we observe an overall decrease in both I_L and ξ toward longer times. This indicates that the population of asphaltene particles is becoming depleted and smaller in size at longer times. At $\phi_m = 0.4$, both I_L and ξ remain roughly constant, indicating that only a relatively small population of asphaltene particles are participating in the aggregation. Finally, we plot the surface scattering parameters, α and I_{surf}, as a function of time, t, for the different ϕ_m in Figs. 8 and 9, respectively. We find that α is small at early times, increases at intermediate times that become systematically longer for larger ϕ_m, and finally saturates at the longest times at a value above 4 for all ϕ_m we
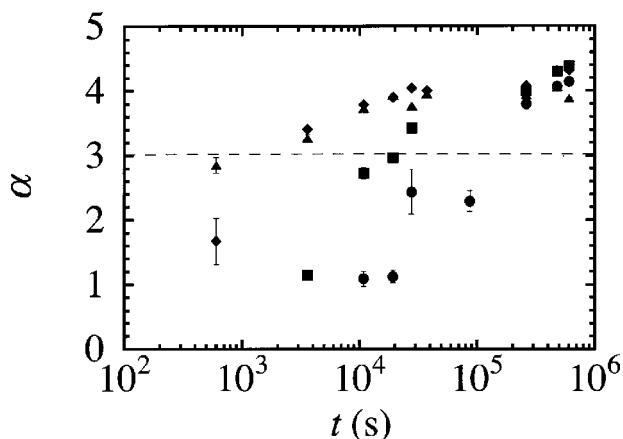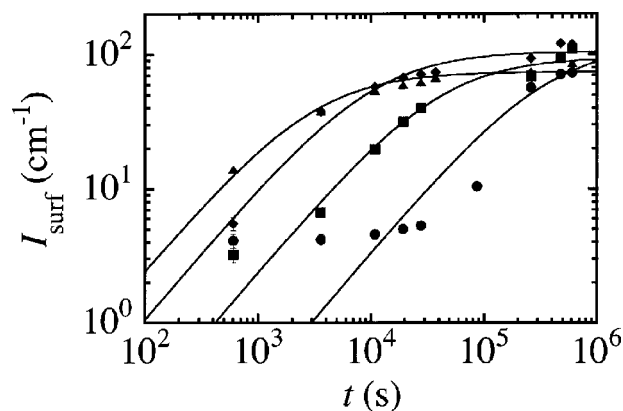
explore. The behavior of I_{surf} over time is qualitatively similar to that of α, as shown in the log–log plot of Fig. 9; however, I_{surf} increases by well over one order of magnitude.

We define a time scale τ_α corresponding to the first appearance of fractal aggregates having at least a size of about 100 nm by determining where $\alpha(t) > 3$, as shown in Fig. 10. We define a different time scale, τ_I, associated with the cessation of the evolution of the aggregation process over a similarly large length scale based on the knee in the growth and long-time saturation of $I_{surf}(t)$, shown for comparison in Fig. 10. To describe the initial increase and subsequent saturation of $I_{surf}(t)$, we have chosen an arbitrary functional form for the fit to be

$$I_{surf}(t) = I_\infty \frac{t/\tau_I}{1 + t/\tau_I}. \tag{2}$$

The fits are shown by the solid lines in Fig. 9; we have excluded the early time data corresponding to an initial constant for $\phi_m = 0.3$ and $\phi_m = 0.4$. We find that the long-time

FIG. 8. The temporal dependence of the surface scattering power law exponent, α, obtained from the fits of the data in Figs. 1–4. The mixing volume fractions are $\phi_m = 0.1$ (triangles), 0.2 (diamonds), 0.3 (squares), and 0.4 (circles). The dashed line $\alpha = 3$ corresponds to fractal surfaces.
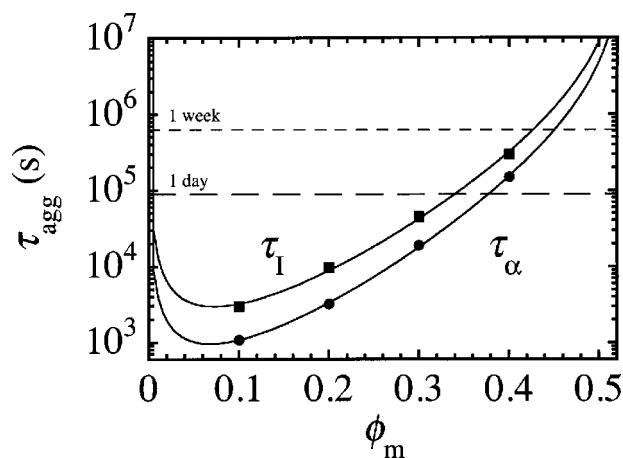
FIG. 10. The characteristic aggregation time τ_α, determined from the criterion $\alpha = 3$ in Fig. 8, and τ_I, determined from the knees in the fits in Fig. 9, as a function of the SACO volume fraction, ϕ_m. The solid lines are fits using Eq. (11) with $d_f = 3$ and $a_0 = 50$ Å, where n_c and ϕ_m^* are allowed to vary. For reference, the dashed lines represent times of one day and one week, respectively.

saturated value of intensity, $I_\infty(\phi_m)$, is approximately independent of ϕ_m so that $I_\infty \approx 100\,\mathrm{cm}^{-1}$ is a good approximation. By contrast, τ_I does exhibit an interesting variation with ϕ_m; we find that τ_I lies systematically two to three times larger than τ_α. This is reasonable since τ_α is more closely associated with the first stages of the aggregation.

V. INTERPRETATION AND DISCUSSION

In order to quantitatively understand the measured increase in aggregation time scales with the mixing volume fraction, we consider a physical model of diffusion-limited aggregation kinetics of asphaltene particles. This model is based on several simplifying assumptions that make the estimate of the time scale feasible, but may not realistically describe the underlying microstructures. The asphaltene particles are considered to be spherical with an average hydrodynamic radius for translational diffusion of $a_0 \approx 50\,\text{Å}$, corresponding to the initial Lorentzian feature in $I(q)$. This neglects the reasonable likelihood that the particles comprised of several planar polyaromatic molecules may be anisotropic in shape. It also neglects the size polydispersity of the particles and the possibility that two large particles may have a deeper attractive well than two small particles. For simplicity, the interaction between all particles is assumed to be very short ranged and much stronger than thermal energy, $k_B T$, where k_B is Boltzmann's constant, so that particles stick irreversibly when they touch. This neglects the possibility for equilibrium gas–liquid and gas–solid phase behavior near the boundary of compatibility that one would expect if the particles could leave the aggregate reversibly due to a relatively shallow attractive potential well.

We model the aggregates of many particles as fractal clusters. The clusters containing n particles also diffuse, but with an effective hydrodynamic radius, a_n, that reflects the fractal dimension of the cluster, d_f:

$$a_n = a_0 n^{1/d_f}, \tag{3}$$

so that a_n grows linearly with n for rodlike clusters having $d_f = 1$ and a_n grows with the cube root of n for compact clusters having $d_f = 3$. For diffusion-limited cluster aggregation (DLCA) of monodisperse spheres that stick with a shear-rigid bond at dilute volume fractions, experiments have shown that $d_f^{\mathrm{DLCA}} \approx 1.75$.[12] Simulations of simple diffusion limited aggregation (DLA) at infinitesimal dilution in which particles aggregate one at a time onto a large cluster yield a larger fractal dimension of $d_f^{\mathrm{DLA}} = 2.5$.

We account for the probability of one cluster encountering a neighboring cluster of the same size after diffusing one intercluster spacing, d_j, where the subscript j refers to the stage of the aggregation and $n = 2^{j-1}$ for simple doubling. We take the encounter probability at stage j, p_j, of a cluster to bond with a cluster of about the same size to be the ratio of the projected hydrodynamic area of six neighboring clusters onto a sphere of area $4\pi d_j^3$. Assuming all spheres are incorporated into clusters of n particles at stage j, the volume fraction of the particles, ϕ, is given by:

$$\phi = \frac{n(4\pi a_0^3/3)}{d_j^3}. \tag{4}$$

This may actually underestimate the intercluster distance, since not all clusters will have precisely size n at the same instant. Solving for the average intercluster spacing, we find:

$$d_j = a_0 \left(\frac{4\pi 2^{j-1}}{3\phi} \right)^{1/3}. \tag{5}$$

Using this value for the spacing, the probability to encounter a neighbor is essentially the square of the cluster radius over the separation:

$$p_j \approx \frac{3}{2}\left(\frac{a_j}{d_j}\right)^2 \approx \frac{3}{2}\left(\frac{4\pi}{3\phi}\right)^{-2/3} 2^{2(j-1)(1/d_f - 1/3)}; \tag{6}$$

for dilute solutions of clusters, the encounter probability can be quite small, reflecting the fact that even though a cluster may diffuse a distance d_j, it may not always find a neighboring cluster of a similar size.

We also hypothesize that the effective interaction potential between two asphaltene particles or clusters includes a repulsive barrier of height U_{rep} at a larger interparticle separation than the essentially infinitely deep short-range attractive well. The probability that thermal energy will drive two clusters together with sufficient energy to overcome the repulsive barrier so that the particles can stick is

$$p_{\mathrm{stick}} = \exp(-U_{\mathrm{rep}}/k_B T). \tag{7}$$

This sticking probability effectively incorporates several different physical effects that may occur when two anisotropic asphaltene particles encounter one another: The first effect is the repulsion that might be present when the aromatic structures of neighboring asphaltenes are oriented at right angles. The second effect is the presence of structures, such as aliphatic side chains or resin molecules, between the asphaltenes that might transiently inhibit their aggregation. We expect that the height of the repulsive barrier will increase with ϕ_m as the solvent quality for the asphaltene particles becomes better and the particles become stable against aggregation. Likewise, we expect $p_{\mathrm{stick}} \to 1$ as $\phi_m \to 0$ because the solvent quality becomes very poor and the particles always stick together when they encounter each other, as in classical DLA.

The characteristic time for two clusters at stage j to diffuse and stick together, t_j, is given by the simple diffusion equation, modified to account for the capture probability:

$$t_j = \frac{d_j^2/(6D_j)}{p_{\mathrm{stick}} p_j}, \tag{8}$$

where the diffusion coefficient is given by the Stokes–Einstein relation:

$$D_j = \frac{k_B T}{6\pi\eta a_0 2^{(j-1)/d_f}}. \tag{9}$$

Here, we have assumed that the convection associated with mixing the two oils together has died out before the aggregation has occurred and that the motion of the clusters is only diffusive. Using Eqs. (3)–(9), the characteristic time to

proceed from aggregation stage $j-1$ to aggregation stage j can be expressed in terms of the fundamental physical parameters:

$$t_j = \frac{2\pi}{3}\left(\frac{4\pi}{3\phi}\right)^{4/3}\left(\frac{a_0^3\eta}{k_BT}\right)\exp(U_{\text{rep}}/k_BT)2^{(j-1)(4/3-1/d_f)}.$$
$$(10)$$

This time is proportional to the viscosity of the solution and inversely proportional to the entropic osmotic pressure of the clusters,[13] so that it diverges as $\phi \to 0$. It grows rapidly with increasing j, and becomes very long for tenuous clusters that have fractal dimensions significantly lower than 3. The presence of a potential barrier stronger than thermal energy can also causes the time to become extremely long.

In order to calculate the total time τ required for aggregation to be completed to length scales larger than SANS probes, we sum all of the the characteristic times t_j up to a critical stage j_c at which the clusters of aggregation number $n_c=2^{j_c-1}$ are significantly larger than the q range we probe. By summing, we implicitly assume that the longest time scale at each stage is set by the diffusion and linking of the largest clusters from the previous stage; this summation ignores the possibility that several smaller clusters than the average may combine to yield large clusters. Assuming $n_c \gg 1$ and using the differential relation $dn/dj=2^{j-1}$, we integrate Eq. (10) over n from $n=0$ to $n=n_c$ and find:

$$\tau = \frac{2\pi}{3}\left(\frac{4\pi}{3\phi}\right)^{4/3}\left(\frac{a_0^3\eta}{k_BT}\right)\exp(U_{\text{rep}}/k_BT)\left(\frac{n_c^{4/3-1/d_f}}{4/3-1/d_f}\right). \quad (11)$$

In Eq. (11), ϕ, η, and d_f may depend on ϕ_m. The parameter n_c is independent of ϕ_m and is essentially set by the length scale of the cluster above which SANS becomes insensitive to further aggregation. We expect this length scale to be of the order of 100 nanometers, since this is several times larger than q_1^{-1} and that it should not depend on ϕ_m, since it reflects the lowest measurable q of the SANS apparatus.

Both the viscosity of the mixture and the volume fraction of particles that will eventually aggregate have been measured as a function of ϕ_m. We assume an empirical functional form for describing the viscosity data in Fig. 5 to be an exponential that incorporates a stretching exponent, γ,

$$\eta(\phi_m)=\eta_0 e^{(\phi_m/\phi_\eta)^\gamma}, \quad (12)$$

where η_0 is the viscosity of the light oil at $\phi_m=0$ and ϕ_η represents the volume fraction of mixing above which the viscosity begins to increase rapidly. The fit to the data using Eq. (12) is shown by the solid line in Fig. 5; it describes the measured viscosity well over the full range of ϕ_m. From the fit, we obtain $\eta_0=4.7$ cP, $\phi_\eta=0.41$, and $\gamma=1.3$. At present, we do not understand theoretically why Eq. (12) describes the measured mixture viscosities.

The total volume fraction of particles available to aggregate has been measured both by SANS and centrifugation. A quadratic form captures the initial rise in ϕ at low ϕ_m due to the addition of more of the asphaltene-containing oil in the bad solvent and the subsequent decrease in ϕ at larger ϕ_m as the solvent quality improves and the oils become more compatible.[7]
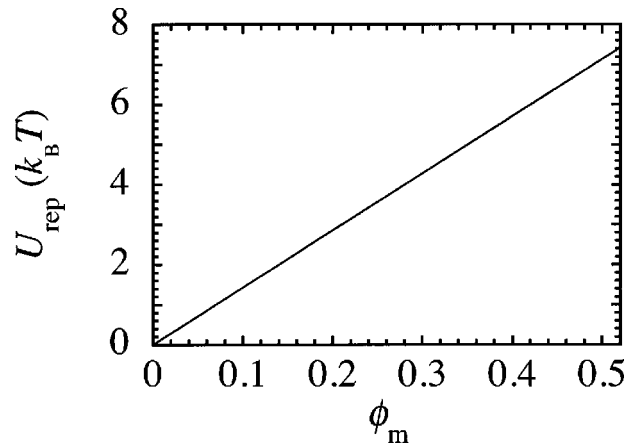

FIG. 11. The estimated repulsive potential barrier height between asphaltene particles, U_{rep}, as a function of the volume fraction of SACO oil, ϕ_m, based on the fits to the data in Fig. 10. The linear increase has been assumed in the model.

$$\phi(\phi_m)=\phi_{\text{SACO}}\phi_m[1-(\phi_m/\phi_c)], \quad (13)$$

where $\phi_{\text{SACO}}=0.12$ is the volume fraction of asphaltene particles in pure SACO oil and $\phi_c=0.53$ is the volume fraction of mixing at which the oils are compatible and no aggregates are observed.

By incorporating the measured $\eta(\phi_m)$ and $\phi(\phi_m)$ in Eq. (11), we fit the SANS measurements of $\tau_\alpha(\phi_m)$ and $\tau_I(\phi_m)$ in Fig. 10 by fixing the fractal dimension to be that of a compact cluster ($d_f=3$), assuming that the repulsive barrier grows linearly with ϕ_m, $U_{\text{rep}}=k_BT(\phi_m/\phi_m^*)$, where ϕ_m^* is the volume fraction of mixing at which the barrier height is equal to thermal energy, and allowing only n_c and ϕ_m^* to vary. The fits, shown by the lines in Fig. 10, describe the measured aggregation times well, and the values of the parameters are $n_c=2.2\times10^5$ and $\phi_m^*=0.068$ for τ_α and $n_c=7.5\times10^5$ and $\phi_m^*=0.074$ for τ_I. These two independent fits yield nearly identical values for ϕ_m^*; this is reassuring since one would expect the sticking probability to be independent of the criteria we have chosen to identify the two different times τ_α and τ_I. From these values of ϕ_m^* and our assumed linear model, we estimate the repulsive barrier height between asphaltenes as a function of solvent quality, and therefore ϕ_m, to be that shown in Fig. 11. At the largest $\phi_m=0.4$ that we have measured, we estimate $U_{\text{rep}}\approx5k_BT$. From the fit, we also deduce that the two values of n_c imply cluster radii of 300 nm corresponding to the definition of aggregation time based on α and 450 nm corresponding to the definition of the aggregation time based on I. These values are reasonable, since they are consistent with the idea that the strong low-q scattering is from the surfaces of compact asphaltene aggregates that are significantly larger than q_1^{-1}. If we allow the aggregates to be less compact, set $d_f<3$, and refit the data, we find that the quality of the fits and the values of ϕ_m^* do not change; instead, n_c increases and the cluster radii become micron scale.

Although this simple model provides good fits to the data using only two adjustable parameters, it does not incorporate all the possible physical parameters that may be important for describing the aggregation time. For instance, we

have completely neglected the polydispersity in the size distribution of asphaltene particles, assuming that all particles are monodisperse with a fixed radius a_0 that does not depend on ϕ_m. Previous measurements of the correlation length of the particles that remain in suspension following mixing indicate that only the largest of the asphaltene particles aggregate near the compatibility boundary, implying that $a_0(\phi_m)$ may actually increase with ϕ_m. This could help account for the longer aggregation times observed as $\phi_m \rightarrow \phi_c$ without the need to introduce as large a potential barrier. Also, the fractal dimension of the asphaltene aggregates may be less than 3, corresponding to clusters that are not completely compact. Moreover, the fractal dimension could depend upon ϕ_m. Finally, we have ignored the possible rearrangement of asphaltene particles once they stick to a cluster, and we have also assumed that asphaltene particles do not reversibly leave the clusters as the solvent quality becomes better. Observations using other techniques, especially real space measurements of asphaltene structures, are needed to further clarify if these numerous assumptions are truly appropriate. For different crude oil mixtures other than those of SACO and BPCO, the scaling prediction of Eq. (11) can serve as a guide for making an initial prediction of the aggregation time. However, a true theory of the DLCA kinetics that includes the polydispersity of the particles, their anisotropic shapes, and the variation in the strength of the barrier height and the depth of the attractive potential well with ϕ_m, is still needed.

VI. CONCLUSION

This study represents the first successful application of TR-SANS as a tool for quantitatively measuring the kinetics of asphaltene aggregation in incompatiable mixtures of crude oils. We have shown that TR-SANS can be used to simultaneously probe the time-dependent growth of the low-q scattering intensity associated with aggregates of asphaltenes as well as the reduction in the average size of the asphaltenes nanoparticles that have not aggregated. Based on the increase and subsequent saturation of $I(q)$ at low q, we have defined characteristic aggregation times for asphaltenes in the crude oil mixtures. Using independent measurements of the vol-

ume fraction of aggregates and the viscosity of the mixtures, we have been able to predict the behavior of the aggregation time as a function of ϕ_m based on simple scaling arguments of cluster aggregation. This prediction yields divergences in τ at $\phi_m = 0$ and $\phi_m = \phi_c$ since no particles are available to aggregate in these limits. To precisely account for the measured increase in the aggregation time from several hours at low ϕ_m to several days at higher ϕ_m, we have hypothesized that there is a repulsive barrier in the average interaction potential between asphaltene particles that depends on the effective solvent quality. By fitting our measurements of the aggregation time as a function of ϕ_m, we have deduced the barrier height $U_{rep}(\phi_m)$. Finally, these measurements clearly show that tests for crude oil incompatibility should be modified to account for the possibility of long aggregation times more than the several days that we have observed.

[1] I. A. Wiehe and R. J. Kennedy, Energy Fuels **14**, 56 (2000).
[2] I. A. Wiehe and R. J. Kennedy, Energy Fuels **14**, 60 (2000).
[3] R. Cimino, S. Correra, A. D. Bianco, and T. P. Lockhart, in *Asphaltenes: Fundamentals and Applications*, edited by E. Y. Sheu and O. C. Mullins (Plenum, New York, 1995).
[4] K. H. Altgelt and M. M. Boduszynski (Marcel Dekker, New York, 1994).
[5] M. Carpineti and M. Giglio, Phys. Rev. Lett. **68**, 3327 (1992).
[6] J. Bibette, T. G. Mason, H. Gang, and D. A. Weitz, Phys. Rev. Lett. **69**, 981 (1992).
[7] T. G. Mason and M. Y. Lin, Phys. Rev. E (to be published).
[8] M. Y. Lin, E. B. Sirota, and H. Gang, Am. Chem. Soc. Div. Fuel Chem. **42**, 412 (1997).
[9] D. Fenistein, L. Barré, D. Broseta, D. Espinat, A. Livet, J.-N. Roux, and M. Scarsella, Langmuir **14**, 1013 (1998).
[10] D. Espinat, E. Rosenberg, M. Scarsella, L. Barre, D. Fenistein, and D. Broseta, in *Structure and Dynamics of Asphaltenes*, edited by O. C. Mullins and E. Y. Sheu (Plenum, New York, 1998), pp. 145–201.
[11] J.-N. Roux, D. Broseta, and B. Demé, Langmuir **17**, 5085 (2001).
[12] M. Y. Lin, H. M. Lindsay, D. A. Weitz, R. Klein, R. C. Ball, and P. Meakin, J. Phys.: Condens. Matter **2**, 3093 (1990).
[13] W. B. Russel, D. A. Saville, and W. R. Schowalter (Cambridge University, Press, Cambridge, UK, 1989).